Enhanced Green Strength Material System for Ferrous and Stainless P/M Processing

Sydney H. Luk, Alan B. Davala, and Howard M. Kopech
Hoeganaes Corporation
Riverton, NJ 08077

Presented at PM2TEC '96 World Congress June 16-21, 1996, Washington, D.C.

ABSTRACT

Strength limitations of green powder metallurgy compacts often present fabricators with processing problems. Increased part complexity, process automation and the need for reduced green scrap requires the P/M compact to attain higher green strength. Currently, several limitations restrict the ability to increase green strength in P/M compacts. Powder characteristics, such as particle size distribution and morphology, compressibility and common lubricant systems, all pose limitations on the compact green strength. Enhanced material systems improve the green strength of ferrous-based P/M parts by a minimum of 100% relative to compacts containing admixed lubricant. Process advantages, specific test results, and side effects of high green strength systems will be discussed.

INTRODUCTION

The green strength of P/M compacts has been studied largely from a powder characteristic or variable approach. Several powder attributes, controlled during the manufacturing operation, have been examined in order to understand and optimize green strength. Klar and Shafer[1] have quantified powder variables affecting green strength into three categories: geometric, intrinsic and surface related factors.

In addition to specific powder attribute studies, several investigations have focused on compaction mechanisms responsible for green strength in P/M compacts. Lurid[2] discounts the mechanism of cold welding for commercial sponge and atomized powder compacts. Instead, he attributes particle interlocking to be the primary source of green strength with increased green strength dependent on the amount of interparticle contact during compaction. Tsuru and Nakagawa[3] investigated the crack formation derived from tooling motion using a 6-axis electric drive CNC press. Their results indicated that cracking in green parts could be avoided by using precise control of tool position and press speed.

German4 describes green strength of a metal powder compact by the following relationship:

$$\sigma = C\,\sigma_o\,\rho^m$$

σ =green strength
C =constant
σ_o = strength of wrought material
ρ = relative density
m= material specific constant

German also relates the green strength to the 'weakest link' theory, relative to the purity of the material surface. Powders with residual oxide layers offer a greater resistance to high green strength formation. Likewise, the introduction of a lubricant to pure, even oxide-free powders presents a barrier or weak link towards developing higher green strength.

In practice, conventional P/M compaction for commercial applications usually requires combinations of metal powders with non-metallic additives. Cold Isostatic Pressing (CIP) and Hot Isostatic Pressing (HIP) offer possible exceptions to this statement. Generally, lubricants, in the form of powder, are admixed with metal powders to assist in the compaction process and protect tooling. The introduction of lubricant to iron powder creates a weak link by establishing a non-metallic interface between the interlocking metal powders. Different lubricant systems offer varying degrees of green

strength for a given density. Figure I show the effect on the green strength of P/M compacts of three common lubricants admixed with an atomized iron powder. Specific characteristics of each lubricant interact differently with the 'geometric' factors of the iron powder, which, in part, determine green strength. Graphite is another common premix additive that will impact the green strength of the compact negatively.

Commercially available iron powders differing in all three factors - geometric, intrinsic, and surface will develop varying levels of green strength. Figure 2 provides a relative comparison of green strength for sponge and water atomized iron, Low alloy and stainless steel powders. Differences in green strength between these powders can be described by one or more factors, similar to those discussed by Klar and Schafer. The reduced green strength of atomized compared with sponge powders, is due mainly to the decreased surface area of atomized powders (i.e. geometric factors). The sponge iron contains internal porosity, which contributes to higher surface areas. Both materials have irregular surface morphologies with Low oxide levels. The further decrease in green strength between atomized iron and Low alloy powders relates to intrinsic factors, such as chemistry and ductility. Carbon and nitrogen decrease the compressibility of iron powders dramatically, as seen by Takajo[5] and Engstrom[6] . As the compressibility of the powder decreases, so does the green strength. Maximizing the compressibility of iron powders is possible by minimizing impurities, and maximizing ductility. This was observed by Lindskog and Arbstedt[?]. Higher levels of particle interlocking will result with increased deformation of ductile iron particles. Luk and Hamill[e] reported that binder treatment of premixes through the ANCORBOND® process increased green strength by 8-25%.

During compaction of a P/M component, the above-mentioned factors collectively influence how well the powder will compact under pressure through particle movement and deformation. Zenget~ et al., and O'Brien~° reviewed the non-destructive inspection methods for detection of green cracks. Bocchini and Schaidl~ have reviewed systematically the relationship between axial and radial pressures developed during the compaction cycle. Further, they discuss the effect of entrapped air within the green compact during compaction, and the internal pressures developed from the compression of the entrapped air. In prior work with Gallo[2], Bocchini determined that the internal pressures due to air compression could reach 7,200 psi (50 MPa). This value of intemal pressures is about twice that of ordinary green strength values, and potentially, could be a factor in developing internal cracking and weakening of the compact.

The objective of the present study was to investigate methods for improving the green strength of PIM compacts, manufactured from commercially available iron powders. By developing an additive designed to lubricate and enhance green strength, a new technology is introduced that allows P/M fabricators to overcome many current production limitations and problems. Performance-driven market requirements with increased mechanical properties necessitate the use of iron powder with additives like copper, nickel, graphite and lubricant, all of which typically reduce green strength in the compact. Fine tooth gears, thin wall sections, and increased use of automated mechanical handling equipment all contribute to the need for increasing the strength of green P/M compacts. Several part geometries are difficult or impossible to compact without cracks, given the current limitations of uniaxial die compaction. Internal cracks developed during the compaction process may be minimized or eliminated with improved green strength of the material. As a result, a new factor that controls green strength can be introduced.

Boundary Surface Treatment

In addition to the conventional particle-interlocking mechanism responsible for green strength, a manipulation of the particle-to-particle boundaries can provide bonding forces, typically 20-30 % above the green strength of die wall lubricated, atomized iron powders. More important is the 100-120% increase in green strength compared with iron PIM compacts produced with conventional admixed lubricants. The weak film of graphite and lubricant between the iron particles is no longer a 'weak link', or a limiting factor. Without a boundary surface treatment, this film reduces the compact strength significantly, relative to the particle-to-particle green strength mechanisms discussed earlier. With practical PIM applications typically requiring additives like graphite and lubricant, the ability to enhance the compact green strength is extremely important. The surface treatment described in the present paper provides a new technology targeted to reduce green scrap and 100% inspection by maximizing the green strength of P/M compacts.

EXPERIMENTAL PROCEDURES

Laboratory testing procedures were carried out in accordance with appropriate ASTM standards. Table I summarize the

powders and premixes studied in this investigation. Laboratory premixes were produced, and green transverse rupture bars (TRS) were compacted and tested according to ASTM B 312. Actual compaction temperature was elevated to 145°F to simulate frictional heat generated during typical production compaction operations. Powders, without internal lubricant, were compacted using zinc stearate die-wall lubricant. The TRS bars were compacted at 30, 40, and 50 tsi (414, 552, 690 MPa).

Metallographic specimens were prepared for optical examination by mounting the green TRS bars in epoxy. Special preparation techniques, including manual polishing, were used to provide an acceptable surface finish.

Production compaction testing was performed to investigate the statistical variability of the compact weight and compaction tonnage. Pilot production premixes were manufactured in 500-pound lots, using a proprietary mixing technique. A cylindrical bushing measuring 1.5 inches in outside diameter, 1.0 inch in inside diameter and 1.5 inches in height was the production test part. The compaction was performed on a Cincinnati 220-ton mechanical press at Cincinnati Technical Center.

Table I - Iron Powder and Premix Compositions

IA	Ancorsteel 1000B$_T$ 0.75 w/o S Lube*
IB	Ancorsteel 1000B~ 0.75 w/o Zinc Stearate
IC	Ancorsteel 1000B
IIA	Ancorstee11000B, 2.0 w/o copper$_T$ 0.8 w/o graphite, 0.75 w/o S Lube*
IIB	Ancorsteel 1000B, 2.0 w/o copper, 0.8 w/o graphite, 0.75 w/o zinc stearate
IIC	Ancorsteel 1000S, 2.0 w/o copper, 0.8 w/o graphite
IIIA	ANCOR 410L, 1.0 w/o S Lube*
IIIB	ANCOR 410L, 1.0 w/o Lithium Stearate

AICan 8081 Copper Powder, Asbury 3203 Graphite, Mallinckrodt Zinc Stearate, Witco Lithium Stearate, * Green Strength Enhanced Lubricant

RESULTS AND DISCUSSION

Green strength is defined as the mechanical strength of an unsintered powder compact. For iron components, the composition typically includes non-metallic constituents, such as graphite and lubricant. Commonly, it is believed that green strength is promoted by the interlocking of the particles during compression. Therefore, the level of green strength depends largely on the initial particle surface asperities. It is enhanced further by the plastic deformation of the metal powder before over-compaction and lamination occurs. The addition of a Low strength material, such as a lubricant, will reduce the green strength if it reduces interlocking of the particles. On the other hand, it may increase green strength if the interlocking of the particles is enhanced through improved density. Additionally, there is the complication of the effect of compaction temperature on the green strength. Most experiments reviewed in the literature were performed at room temperature rather than at production compaction temperatures. During compaction, the heat generated by friction between the particles and against the die wall is significant. The temperature of the green compact can range from 80°F to 200°F. In the present study, all test specimens were compacted at a temperature of 145°F to simulate production conditions.

Effect of Lubricant Addition on Green Strength

Initially, the green strength of atomized iron powder with no alloying additions was investigated to provide a better understanding of how admixed and die-wall lubricants contribute to the green strength of the compact. The physical and green properties of the materials under investigation are listed in Table II. Compositions of Materials IA, IB and IC were presented in Table I. In Material IA, an addition of 0.75 w/o S lube was made through the new green strength premix technology. In Material IB, 0.75 w/o zinc stearate was admixed to the iron powder. The reference Material IC is composed only of atomized iron particles. Zinc stearate was sprayed on the tooling surfaces prior to compaction. The effect of these lubricants on the green strength of TRS bars compacted at 30, 40 and 50 tsi is shown in Figure 3. The green strength for the die-wall lubricated powder (IC) increased from 4,600 psi to 8,300 psi as compaction pressure increased from 30 tsi to 50 tsi. Correspondingly, the green strength for the powder (IB) lubricated with admixed zinc

stearate increased from 2,500 psi to 3,100 psi. This confirmed the conventional thinking that the admixed lubricant reduced green strength by forming a weak bond between the iron particle surfaces. The green strength of the compact is governed by its weakest structural feature and not by the strength of the actual solid material. For the zinc stearate lubricated powder (IB), the weakest structural surface is that between the lubricant particles and the iron particles. This is a rather weak bond such that under sufficient stress, the green compact simply will fracture in a brittle manner. As the compaction pressure is increased to 50 tsi, the lubricant particles are deformed forming a solid film that is squeezed between the iron particles.

The additional compaction pressure also increases the particle-to-particle interlocking, increasing the green strength from 2,500 psi to 3,100 psi.

For the die-wall-lubricated powder (IC), the weakest structural feature is the interlocking surface between the iron particles. This forms a much stronger bond than that of the lubricated powder. As the compaction pressure is increased to 50 tsi, the iron particles plastically deform, increasing the green strength from 4,600 psi to 8,300 psi. A further increase in the compaction pressure may result in laminations within the compact.

The green strength curve for the powder lubricated with the green strength enhancer (IA) resembled that of the die-wall lubricated material (IC), but at higher green strength values. The green strength increased from 5,500 psi to 8,800 psi. At first glance, this result appears contrary to conventional thinking suggesting that the lubricated powder has a stronger bond between the interlocking surfaces than that of die-wall lubricated powder. Additionally, the response to higher compaction pressure is similar to that for Material IC. One explanation is that the powder lubricated with the green strength enhancer provides superior internal lubricity, improving the green density of the compact significantly.

Comparing the curves of Materials IA and IC, it takes much higher compaction pressure for the die-wall-lubricated powder to reach the same green strength. For example, to attain a green strength of 5,600 psi, a compaction pressure of 36.2 and 30.8 tsi is required for Materials IC and IA, respectively. A maximum green strength of 3,100 psi was obtained with the internally lubricated Material IB, by applying a compaction pressure of 50 tsi.

Effect of Lubricant Addition on Compressibility

The compressibility curves of the three mixes are shown in Figure 4. Overall, the compressibility of Material IA is superior to both Materials IB and IC. Yamton and Davies[3] defined the presence of · crossover point between admixed and die-wall lubricated powders. Hershberger and McGeehah[4] discuss the presence of a crossover point between internally and externally lubricated high purity water atomized iron powders. The cress-over point depends on both testing conditions and the compressibility of the material system. The existence of a cress-over point between the die-wall lubricated Material IC and Material IB with admixed lubricant, suggests the possibility of an optimum lubricant content to minimize pressure loss due to friction. As expected, the compressibility of the die-wall lubricated Material IC is less than that of the lubricated materials IA and IB until the crossover point. At compaction pressures higher than the crossover point, the lubricant itself is compressed during compaction. The volume compression of the zinc stearate causes the springback of the lubricated powder compacts to be higher than that of a die-wall lubricated powder. At 50 tsi, the green expansion for Material IC is 0.00% versus 0.10% for Material IB. The presence of admixed zinc stearate will increase internal stresses contributing towards cracking of compacts. It should be noted that material with some admixed lubricant always exhibits a better response to densification than a material without admixed lubricant. For compacts with multiple levels and difficult shapes, densification requirements and compressibility should be considered. Comparing Materials IA and IC, there is no crossover point. Both curves converge at the compaction pressure of 50 tsi. The compressibility of Material IA is much higher than Material IC. For Material IA, the green expansion is 0.03% at 50 tsi, and only 0.01% at 40 tsi. This springback is equivalent to that of the pure iron with die-wall lubricant, and significantly less than that of the Material IB.

Pore-Free Density (PFD)

It is common to view the compressibility of powders from a density viewpoint. Density is the ratio of the mass of a powder to the volume of the compact. It does not indicate the fraction of volume occupied by solid masses and voids. The relationship between void space and green strength may be important. Viewing the green compact from a volume or void space point of view can prove insightful. The pore-free density (PFD) is defined as the density achieved if all void

spaces in the compact are eliminated. The ratio of the green density to the pore-free density is defined as % PFD. Hence, a compact with 98% pore-free density means that there exists a two-volume percent of voids within the compact.

The pore-free densities for selected materials are listed in Table III. The compressibility curves, previously discussed for Materials IA, IB, and IC in Figure 4, have been re-plotted as % PFD versus compaction pressure and are shown in Figure 5. On the basis of volume, Figure 5 shows that the compaction of powders with admixed lubricant and the die-wall lubricated powders follow a different trend. Material IA is more compressible at higher compaction pressures reaching a 98.1% PFD at 50 tsi. Comparatively, at 50 tsi, Materials IB and IC reached 97.3% PFD and 93.2% PFD, respectively. Percent void space can be defined by the following relationship:

$$\% \text{ Void Space} = 100 - \% \text{ PFD}$$

On a volume basis, Material IC has 6.8% void space even though it reached a green density of 7.31 g/cm^3 at 50 tsi. The powders with admixed lubricant have 1.9 to 2.7% void spaces.

The relationship between green strength and green density is shown in Figure 6. It shows that for a constant green strength of 8,000 psi, the green density for Material IA is 7.23 g/cm^3 and 7.27 g/cm^3 for Material IC, a difference of 0.04 g/cm^3. The relationship between green strength and % PFD is shown in Figure 7. At constant % PFD, the green strengths of Materials IC and IA are greater than Material IB.

At a constant green strength of 8,000 psi, the % PFD for Material IC is 92.7%, and 96.7% for Material IA. This means that the difference in void space between the powder lubricated with the green strength enhancer (IA) and die-wall lubricated powder (IC) is 4 v/o. This 4 v/o represents the space occupied by the lubricant in the Material with a green strength of 8,000 psi. At a lower green strength value of 5,600 psi, there is a difference of 3.75 v/o between Materials IA and IC. The rate of increase in green strength with respect to % PFD is similar for both Materials IA and IC, indicating that the mechanism providing the higher green strength in IA is similar to that in IC in terms of total void volume. As the void volume decreases, deformation and interlocking of the particles is increased.

This is contradictory to conventional thinking. Material IA is composed of iron particles and 0.75 w/o of S lubricant particles. Actually, the lubricant particles are enhancing the green strength rather than impeding it. For Material IB, the rate of increase with respect to % PFD is minimal. Material IB is composed of 0.75 w/o of zinc stearate particles and iron particles. In this case, the lubricant is impeding the rate of increase of green strength with % PFD when compared with the die-wall-lubricated powder (IC). At 92% PFD, the green strength achieved by Material IB is 2,400 psi compared with 5,600 psi achieved by Material IA.

Stripping and Sliding Pressure

The force required to eject a compact from the die cavity can be measured in terms of stripping pressure and sliding pressure as described by Luk and Hamills. Stripping pressure is the force required to overcome friction when the initial ejection process begins. Sliding pressure is the force required to overcome frictional forces while the compact is moving during ejection. In Figure 8, the stripping pressure required to eject the compact for Materials IA, IB and IC is compared at different compaction pressures. In Figure 9, the corresponding sliding pressure is plotted against the compaction pressures. Material IC required the highest stripping and sliding pressure compared with Materials IA and IB. The powders with admixed lubricant, Materials IA and IB followed a similar trend with respect to increasing compaction pressure. Material IA required the lowest stripping and sliding pressure for ejection. This indicates that Material IA had better external lubricity than Materials IB and IC.

Microstructures of the Green Compacts

The green compacts of Materials IA, IB and IC pressed at 50 tsi were investigated with respect to particle-to-particle interlocking. Sections were cot from the TRS bars, epoxy impregnated, and pressed into 1.25-inch Metallographic mounts. Due to the soft nature of the green compacts, the samples were prepared by vibratory polishing. This was done to maintain sample integrity and to avoid pullout. Optimum viewing of the samples was in the unetched condition. Figures 10, 11 and 12 show the condition of the green compacts near the die-wall. Comparing Figures 10 and 11 dearly indicates a different interlocking pattern near the die-wall between Materials IB and IA. The microstructure for Material

IA is similar to that of Material IC. The microstructure for the die-wall lubricated powder IC is shown in Figure 10. At the die-wall region, the oblique illumination technique was used to show the surface region. A 40-micrometer wide boundary layer exists with few or no pores visible. 'Flow lines' are visible within this region, formed by the deformation and movement of the powder along the die-wall. The microstructure resembles the flow pattern of a highly viscous mass moving along a wall. It should be noted that there is no encapsulation of any die-wall lubricant, which would have resulted in visible pores or crack lines. During compaction with die-wall lubrication, the single layer of iron particles in contact with the wall was lubricated. This increased the local compressibility of this first layer, while the second layer of particles continued to deform without the aid of lubricant.

The 20 to 40 micrometers region, seen in Figure 10, corresponds to a single layer of iron consisting of one or two particle diameters. During ejection, the powder mass in contact with the die-wall is sheared in the direction of ejection. The compact is restricted radially by the die-wall and the static friction between the die and compact surfaces dictates the stripping force required moving the compact. The high stripping pressure of 6,600 psi recorded for Material IC indicates there is insufficient lubricant remaining at the die surface for material ejection. A high sliding pressure of 3,100 psi was recorded. The deformed particles near the die-wall are subject to the internal stresses of the compact. The particles further away from the boundary layer are highly interlocked with each other resulting in very fine particle-to-particle boundaries.

The microstructure of Material IB is shown in Figure 11. There are no boundary layers or 'flow lines' near the die-wall and there are voids close to the die-wall, partially occupied by the lubricant particles. During ejection of the compact, these lubricant particles will continue to lubricate the die surface. This results in lower stripping and sliding pressures of 4,500 psi and 2,200 psi, respectively. The particles further away from the die-wall show much less interlocking. Zinc stearate particles are either deformed to form a solid film and squeezed between the iron particles or just occupies void space between deformed iron particles. This is shown in Figure 13, where the arrow marker indicates the location of the zinc stearate. For the powder admixed with zinc stearate (IB), the weakest structural surface is between the lubricant particle and the iron particle. This results in a Lower green strength of 3,100 psi.

The microstructure of Material IA is shown in Figure 12. This structure is quite similar to that of Material IC. There is a boundary layer and similar "flow line" at the die-wall interface. The particles further away from the boundary layer are highly interlocked resulting in very fine particle-to-particle boundaries. This results in the high green strength of 8,800 psi. There are no large voids partially occupied by the lubricant as in the case of Material IB.

The core regions of the green compacts are shown in Figures 14, 15 and 16. For Material IC shown in Figure 14, there is a high degree of particle interlocking. This is indicated by the very fine particle-to-particle boundaries. The number of large voids is limited and there are no lubricants occupying the space between iron particles. A lack of particle rearrangement during compaction can be seen by the patterns of the particle boundaries. The particles are compressed on top of each other. There is no internal lubricant to allow the particles to slide and rearrange into the optimum packing order. Zinc stearate particles are visible in Material IB (Figure 15). The lubricant occupies the large void spaces between iron particles. This results in less iron-to-iron particle interlocking. It is also evident that there was particle rearrangement during compaction. In Figure 16, Material IA showed a unique microstructure. There are no large voids occupied by the lubricant as in Figure 15, and the particle boundaries are very fine, indicating a high degree of interlocking and particle rearrangement. The net result is a very high green strength compact.

Sintered Properties

Sintered property testing was conducted to compare the effect of admixed green strength enhanced S lubricant (IA) with Material IB admixed with zinc stearate. The results are summarized in Table IV. At constant compaction pressures, the sintered density and apparent hardness values of Materials IA and IB are similar. The sintered TRS for Material IA is lower than that of Material IB. At a compaction pressure of 40 tsi, the TRS value for Material IA is 75,000 psi versus 78,000 psi for Material IB. At a compaction pressure of 50 tsi, the TRS values are 80,500 and 104,300 psi, for Materials IA and IB, respectively. If necessary, the 10-20% reduction in sintered strength can be recovered by alloy or processing adjustments. The new green strength enchanced material was designed to improve compact green strength for complicated shapes and fine tooth gears that typically experience cracking or chipping problems. However, future research will be conducted to minimize any differences in sintered properties between conventional admixed lubricants and the enhanced green strength lubricant while maintaining the benefit of higher green strength.

Effect of Alloy Additions on Green Strength

Materials IIA, IIB, and IIC, in Table I, represent an FC-0208 composition. The physical and green properties are summarized in Table I1. The effect of lubrication method and alloy additions on the green strengths of compacts at 30, 40 and 50 tsi is shown in Figure 17. The green strength for the die-wall lubricated Material IIC increased from 3,500 psi to 5,400 psi as the compaction pressure increased from 30 tsi to 50 tsi. This is significantly lower than the green strength of Material IC. The decrease can be attributed to the graphite addition. Graphite is a lubricant and occupies space between the iron particles. However, the effect is less detrimental compared with that of the zinc stearate. The effect of admixed copper on green strength is also negative. The strength provided by the interlocking of a copper particle and an iron particle is expected to be lower than that of two iron particles. Correspondingly, the green strength for Material IIB, is even lower. Material lib only increased in green strength from 2,300 psi to 2,700 psi, confirming the conventional thinking that both the admixed lubricant and graphite reduce green strength by forming a weak bond between the iron particle surfaces.

For Material IIA, the green strength curve resembles that of Material IIC, but at significantly higher green strength values. The green strength increased from 5,300 psi to 6,800 psi as compaction pressure increased from 30 tsi to 50 tsi. This indicates that Material IIA has a stronger bond between the interlocking particle surfaces than material IIC. At a compaction pressure of 30 tsi, the green strength value of 5,300 psi is comparable to that of the die-wall lubricated iron, Material (IC), which has neither graphite nor copper additions. This indicates that the green strength enhanced Material IIA is offsetting the negative effect of both graphite and copper on green strength at Low compaction pressure.

In producing a compact of complex shape, it is precisely the green strength in the region of Low effective compaction pressure that is of critical importance. Material IIA will provide sufficient green strength in such cases. One explanation for the improved green strength is that Material IIA provides superior internal lubricity causing the green density of the compact to improve significantly. The compressibility curves of the three materials are shown in Figure 18. Comparing Materials IIC and IIB, a crossover point exists at a compaction pressure around 35 tsi. Comparing the curves of Material IIA and Material IIC in Figure 18, it takes much higher compaction pressures for Material IIA to reach the same green density after the cross-over point. This shows that the addition of graphite and copper impedes the densification process for both Materials IIA and IIB. However, Material IIA is still more compressible than Material IIB.

The relationship between green strength and green density is shown in Figure 19. At a constant green strength of 5,200 psi, the green density for I1A is 6.86 g/cm^3 and 7.29 g/cm^3 for IIC. The difference of 0.49 g/cm^3 is ten times the density difference between Materials IA and IC.

The relationships between green strength and % PFD for Materials IIA, IIB, and IIC are showed in Figure 20. At a constant % PFD, the green strength of Materials IIC and IIA is significantly higher than that of Material IIB. At a constant green strength of 5,200 psi, the %PFD for Material IIC is 95.3% compared with 93.6% for Material IIA. This is a difference of only 1.7 v/o. The addition of graphite and copper powder increased the %PFD achieved by Material IIC, compared with that of Material IC. Conversely, it reduced the amount of void space significantly. The 1.7 v/o represents the space occupied by the lubricant, at a green strength level of 5,200 psi. Previously, at a green strength value of 5,600 psi, there was a difference of 3.75 v/o between Materials IA and IC. Adding the graphite and copper powder resulted in a reduction of 2.05 v/o in void space occupied by the lubricant. The rate of increase in green strength with respect to % PFD is similar for both Materials IIA and IIC, indicating that the mechanism providing the higher green strength in Material IIA is similar to that in Materials IIC in terms of total void volume. As the void volume decreases, the particles increasingly deform and interlock with each other. The lubricant particles in Material IIA actually are enhancing the green strength further with the addition of graphite and copper particles. However, for Material IIB, the rate of increase with respect to % PFD is minimal. Material lib is composed of 0.75 w/o of zinc stearate particles, graphite, copper and iron particles. In this case, zinc stearate, copper and graphite are impeding the rate of increase of green strength with % PFD when compared with Material IIC.

The stripping and sliding pressures are plotted with respect to compaction pressures in Figures 21 and 22. Material IIC required the highest stripping and sliding pressure compared with Materials lib and IIA. Material IIA required the lowest stripping and sliding pressure, indicating that Material IIA provided better external lubricity than Materials lib and IIC. However, the ejection performance for Material IIC is significantly better than Material IC. In other words, copper and

graphite assist both as external and internal lubricants.

Sintered Properties

Sintered property testing was conducted to compare the effect of admixed green strength enhanced lubricant with that of admixed zinc stearate, for FC-0208 materials. At constant compaction pressure, the sintered density and apparent hardness values of Materials IIA and lib are similar. The sintered TRS for Material IIA is lower than that of Material lib by 4-10%, depending on density. At a compaction pressure of 50 tsi, the TRS value for IIA is 169,000 psi versus 189,000 psi for Material IIB. As discussed earlier, the main focus of the enhanced green strength material was towards improvement of the integrity of green compacts. For most applications, the 4-10% decrease in sintered TRS for a FC-0208 material is negligible. Further work is being conducted to improve the sintered strength of green strength enhanced materials.

Green Strength of 410L

The effects of the green strength enhanced lubrication on 410L stainless powder was investigated. The original testing was carried out in connection with a specific application, requiring compaction pressures of 50 tsi. Therefore, the data and results currently are limited to this tonnage. Future work will include testing at 30, 40 and 50 tsi (414, 552, 690 MPa).

The compositions of Materials IIIa and IIIB are listed in Table I. Table II contains the physical and green properties of 410L admixed with 1.0 w/o lithium stearate and 410L admixed with 1.0 w/o S lube. When compacted at 50 tsi, the green strength of the S lubricated premix increases more than 3.5 times relative to the lithium stearate lubricated premix. A slight improvement in stripping and sliding pressure is observed with Material IIIA. The same mechanisms discussed for Material IA apply to the 410L material. However, the difference in particle morphology and particle size distribution of the 410L powder relative to the
Ancorsteel 1000B used in Materials IA and IIA, causes the apparent density to change. The apparent density of the S lubricated 410L powder decreased substantially. Additional research is required to minimize this difference in actual production applications. Decreasing the addition from 1.0 w/o to 0.75 w/o will provide some improvement. Table IV contains the sintered property results and reference to the sintering conditions. A slight decrease in all sintered properties was observed. However, neither the dimensional change, rupture strength, nor hardness reductions appear particularly significant.

Production Compaction Trials

The previous sections of this investigation focus on the fundamentals of green strength enhancement. The balance will focus on validation of this technology, in terms of production compaction capability.

Compaction studies were carried out on a 220-ton Cincinnati mechanical press. The variability of part weight and compaction tonnage were examined. An FC-0208 composition, Material IIA containing the S lube, and a reference premix were tested at 40 and 50 tsi. The reference material was the same composition as Material IIB, except it contained 0.75 w/o Acrewax instead of the zinc stearate employed in the laboratory trials. Five hundred test cylinders were compacted from each material without press or tooling adjustments during the compaction cycle. Table V lists the mean and standard deviation results for part weight and compaction tonnage. The green strength enhanced materials showed 21-24% decreases in part weight variation, and a 19-36% reduction in tonnage variation for the FC-0208 composition compared with the reference mix. The 410L stainless material with green strength enhancement showed an 8.5% decrease in part weight variation, and a 27.5% reduction in tonnage variation.

Table V: Production Variability

Material	Part Weight		Compaction Tonnage (tsi)	
	Mean	Std Div	Mean	Std Div
IIA - 0.75 w/o S Lube 40 tsi	117.94	0.274	39.23	0.58
IIB - 0.75 w/o Actawax 40 tsi	110.76	0.334	41.24	0.79
IIA - 0.75 w/o S Lube 50 tsi	118.03	0.280	49.99	0.84
IIB - 0.75 w/o Acrewax 50 tsi	109.95	0.349	51.32	1.00
410L + 1.0 w/o S Lube	22.3	0.071	55.5	0.367
410L + 1.0 w/o LiSt	25.7	0.085	56.7	0.468

CONCLUSIONS

A new material system developed to enhance the green strength of iron, Low alloy and stainless steel powders is presented. The green strength enhancement lubricant does not contain zinc or other additives that present environmental concerns. The mechanism responsible for green strength enhancement is investigated through microstructure and void volume analysis. The degree of interlocking between various surfaces is responsible for the green strength enhancement. Improvements in green strength greater than 100% were achieved in pure iron, an FC-0208 composition, and 410L stainless materials. These enhancements in green strength far outweigh the decrease in sintered strength observed. Sintered density and apparent hardness are near parity with conventionally admixed lubricants.

Production trials have demonstrated that the new green strength enhancer is suitable for commercial application. Specifically, premixes manufactured with the green strength enhancer reduced compaction tonnage and part weight variation by 22 and 28%, respectively.

ACKNOWLEDGMENT

The authors are very grateful to T. Murphy for the microstructural analysis of the green compacts. We would also like to acknowledge P. Kramus, H. Phan and F. Chan for their input in this work.

REFERENCES

1. Klar, E., Shafer, W.M., "On Green Strength and Compressibility in Metal Powder Compaction", Modem Developments in Powder Metallurgy-1976, Vol. 9, compiled by Henry H. Hausner & Pierre W. Taubenblat, pp. 91-113, Metal Powder Industries Federation, Princeton, NJ.

2. Lund, J.A., "Origin of Green Strength in Iron Compacts", Int. J. PowderMetall. Powder Technol., Vol. 18 (No. 2), 1982, pp 117-127.

3. Tsuru, T., Nakagawa, T., "Studies in Crack Formation in P/M Compacting", Advances in Powder Metallurgy and Particulate Materials -1992, Vol. 2, compiled by Joseph M. Capus and Randall M. German, pp. 291-300, Metal Powder Industries Federation, Princeton NJ.

4. German, R.D., Powder Metallurgy Science, Second Edition, 1994, pp 222-224, Metal Powders Industries Federation, Princeton, NJ.

5. Takajo, S., "innovations in Ferrous Powders and Their Production", Powder Metallurgy, July 1986, State of the Art Powder Metallurgy in Science and Practical Technology, Vol. 2, Editors W.J. Huppmann,W.A. Kaysser and G. Petzow, Published by Vetlog Schmid, GmbH, Freiburg, pp 11-39.

6. Engstr6m, U.,"lnnovations in Ferrous PM", Powder Metallurgy, July 1986, State of the Art Powder Metallurgy in Science and Practical Technology, Vol. 2, Editors W.J. Huppmann, W.A. Kaysser and G. Petzow, Published by Verlog Schmid, Grabri, Freiburg, pp 41-70.

7. Lindskog, P.F., Arbstedt, P.J., "Iron Powder Manufacturing Techniques: A Brief Review", Powder Metallurgy, Vol. 29, No. 1, pp 14-19.

8. Luk, S.H., Hamill, J.A., "Dust and Segregation-Free Powders for Flexible P/M Processing", Advances in Powder Metallurgy and Particulate Materials - 1993, Vol. 1, compiled by Alan Lawley & Armour Swanson, pp 153-168, Metal Powder Industries Federation, Princeton, NJ.

9. Zenger, D.C., Ludwig, R., Zhang, R., McCabe, L., "Detecting Cracks in Green P/M Components", Advances in Powder Metallurgy and Particulate Materials - 1995, Vol. 3, compiled by Marcia Phillips & John Porter, pp 9-16, Metal Powder Industries Federation, Princeton, NJ.

10. O'Brien, R.C. and James, W.B., "A Review of Nondestructive Testing Methods and Their Applicability to Powder Metallurgy Processing", MPIF Seminar on Prevention and Detection of Cracks in Ferrous P/M Pads, 1988, International Powder Metallurgy Conference and Exhibition.

11. Bocchini, G.F., Schaidl, H., 'Powder and Mix properties, Tooling and Innovative Presses, Suitable to Avoid Cracks in P/M Part Compacting', Advances in PowderMetallurgy- 1991, Vol. 1, compiled by Leander F. Pease III & Reynald J. Sansoucy, pp 59-88, Metal Powder Industdes Federation, Princeton, NJ.

12. Bocchini, G.F., Gallo, A., "La Lubdficazione Nella Pressatura Delle Ploved Metalliche", AIM, Convegno Nazionale de Tribologia, Milano, September, 1983.

13. Yamton, D. and Davies, T.J., "The Effect of Lubrication on the Compaction and Sintedng of Iron Powder Compacts", International Journal of Powder Metallurgy 8 (2), 1972, p 51.

14. Hershberger, R.H., McGeehan, P.J., "A New Higher Compressibility Iron Powder", progress in Powder Metallurgy-1986, Vol. 42, compiled by Earl A Cadson & Gary Gaines, pp 305-320, Metal Powder Industdes Federation, Princeton, NJ.

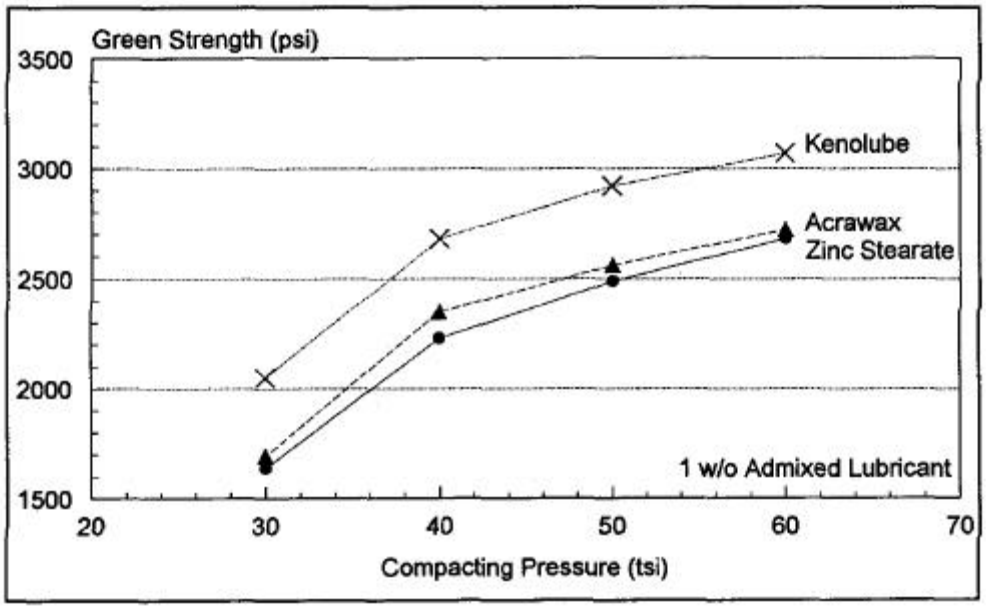

Figure 1: Green Strength of an Atomized Iron with 1 w/o Lubricant

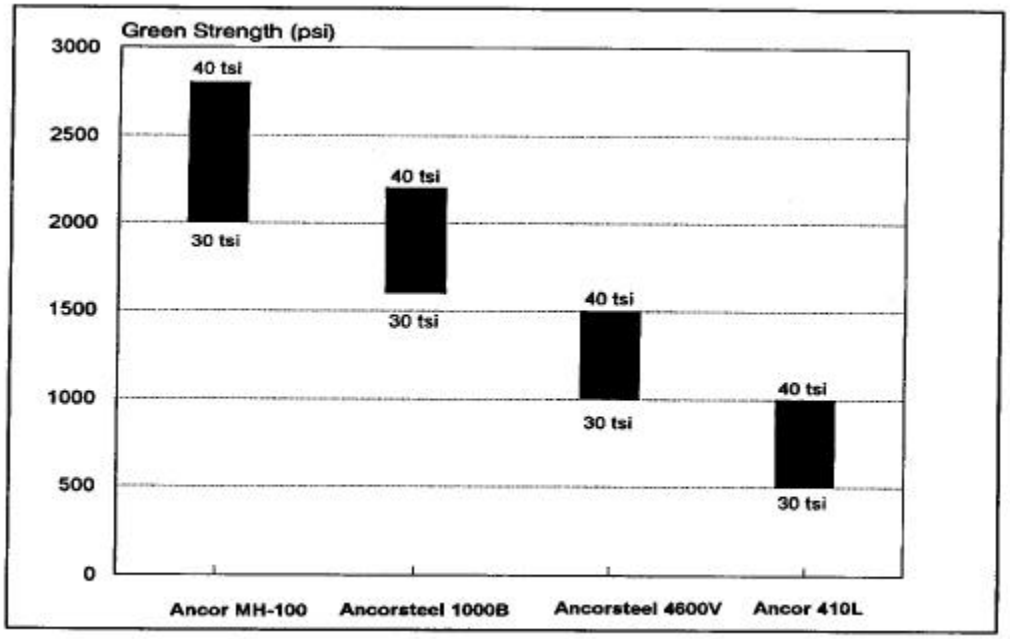

Figure 2: Green Strength of Various Iron Powders with 1 w/o Lubricant

Table II: Physical and Green Properties

Material	Apparent Density (g/cm³)	Flow (s/50g)	Compaction Pressure (tsi)	Green Density (g/cm³)	Green Strength (psi)	Strip Pressure (psi)	Slide Pressure (psi)	Green Expansion (%)
IA	2.90	24	30	6.84	5472	2949	1361	-0.01
			40	7.16	7378	4113	1433	+0.01
			50	7.32	8790	4367	1602	+0.03
IB	3.26	26	30	6.84	2513	3621	1767	+0.02
			40	7.12	2953	4357	2319	+0.06
			50	7.26	3133	4473	2237	+0.10
IC	2.94	24	30	6.72	4597	5097	4428	+0.01
			40	7.05	6258	7530	4156	+0.01
			50	7.31	8328	6609	3118	0.00
IIA	2.89	28	30	6.86	5281	2368	1094	+0.04
			40	7.12	6471	2884	1166	+0.07
			50	7.22	6823	3114	1205	+0.09
IIB	3.22	30	30	6.88	2268	3403	1097	+0.03
			40	7.09	2621	3280	1452	+0.08
			50	7.19	2748	3697	1585	+0.11
IIC	2.91	28	30	6.83	3546	4122	1994	0.00
			40	7.14	4530	4044	1684	+0.07

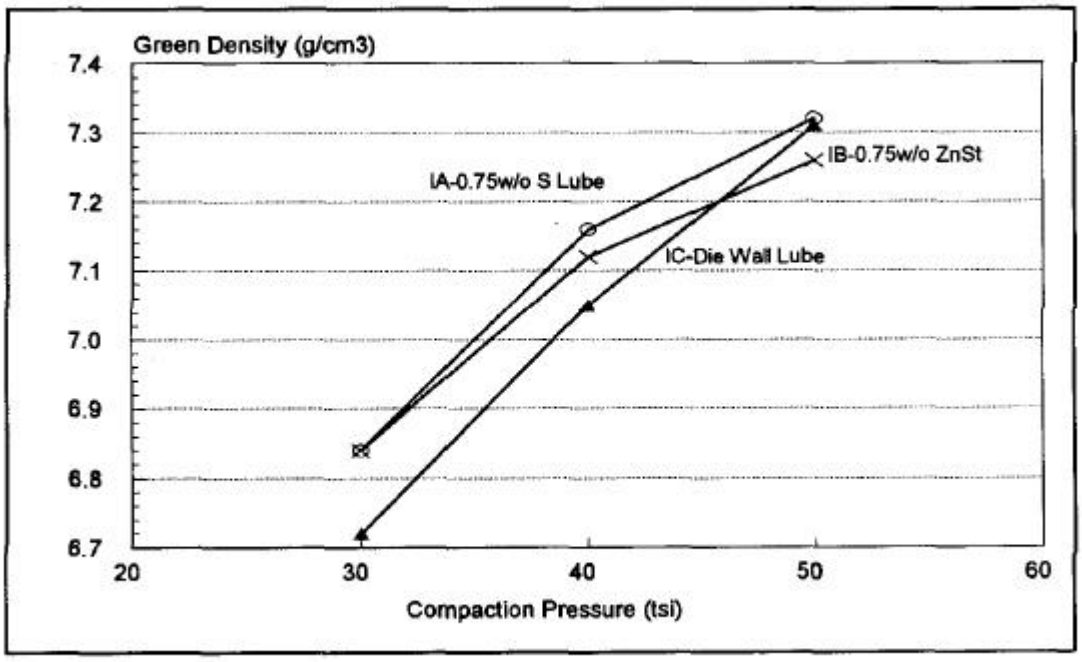

Figure 4: Compressibility of Ancorsteel 1000B with 0.75 w/o Admixed S Lube,

Table III: Pore-Free Density Values

Material	Pore Free Density	30 tsi 414 (MPa)	40 tsi 552 (MPa)	50 tsi 690 (MPa)
IA	7.46	6.84	7.16	7.32
	100%	*91.7*	*96.0*	*98.1*
IB	7.46	6.84	7.12	7.26
	100%	*91.7*	*95.4*	*97.3*
IC	7.84	6.72	7.05	7.31
	100%	*85.7*	*89.9*	*93.2*
IIA	7.33	6.86	7.12	7.22
	100%	*93.6*	*97.1*	*98.5*
IIB	7.33	6.88	7.09	7.19
	100%	*93.9*	*96.7*	*98.1*
IIC	7.67	6.83	7.14	7.33
	100%	*89.0*	*93.1*	*95.6*

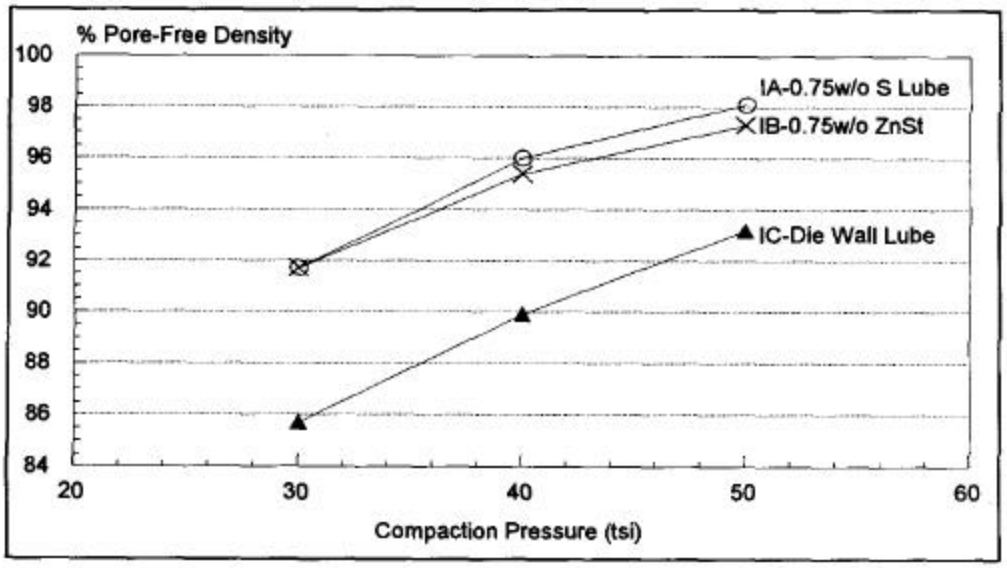

Figure 5: Percent Pore-Free Density of Ancorsteel 1000B with 0.75 w/o Admixed S Lube, 0.75 w/o Admixed ZnSt, and ZnSt Die-Wall Lubricant

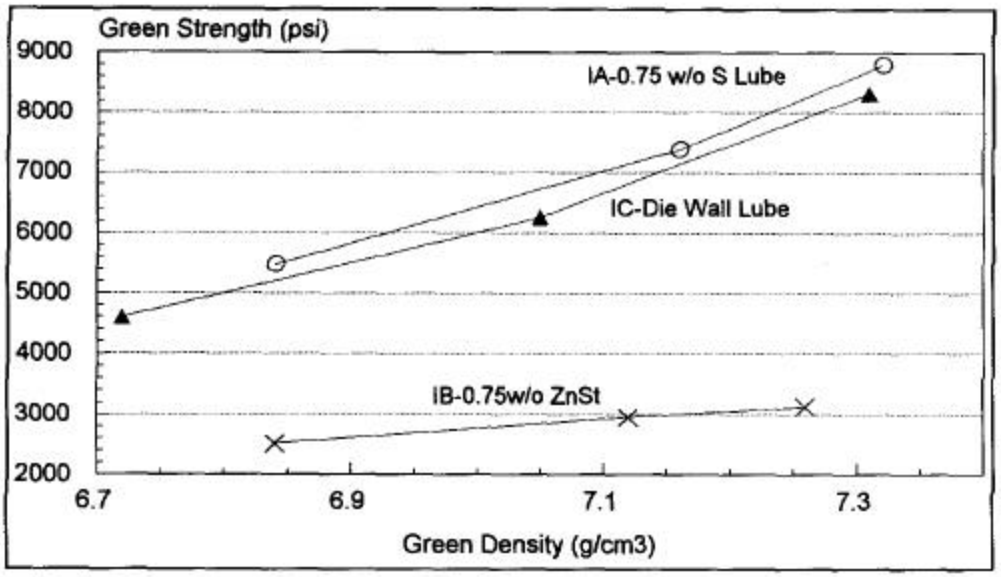

Figure 6: Green Strength as a Function of Green Density of Ancorsteel 1000B with 0.75 w/o Admixed S Lube, 0.75 w/o Admixed ZnSt, and ZnSt Die-Wall Lubricant

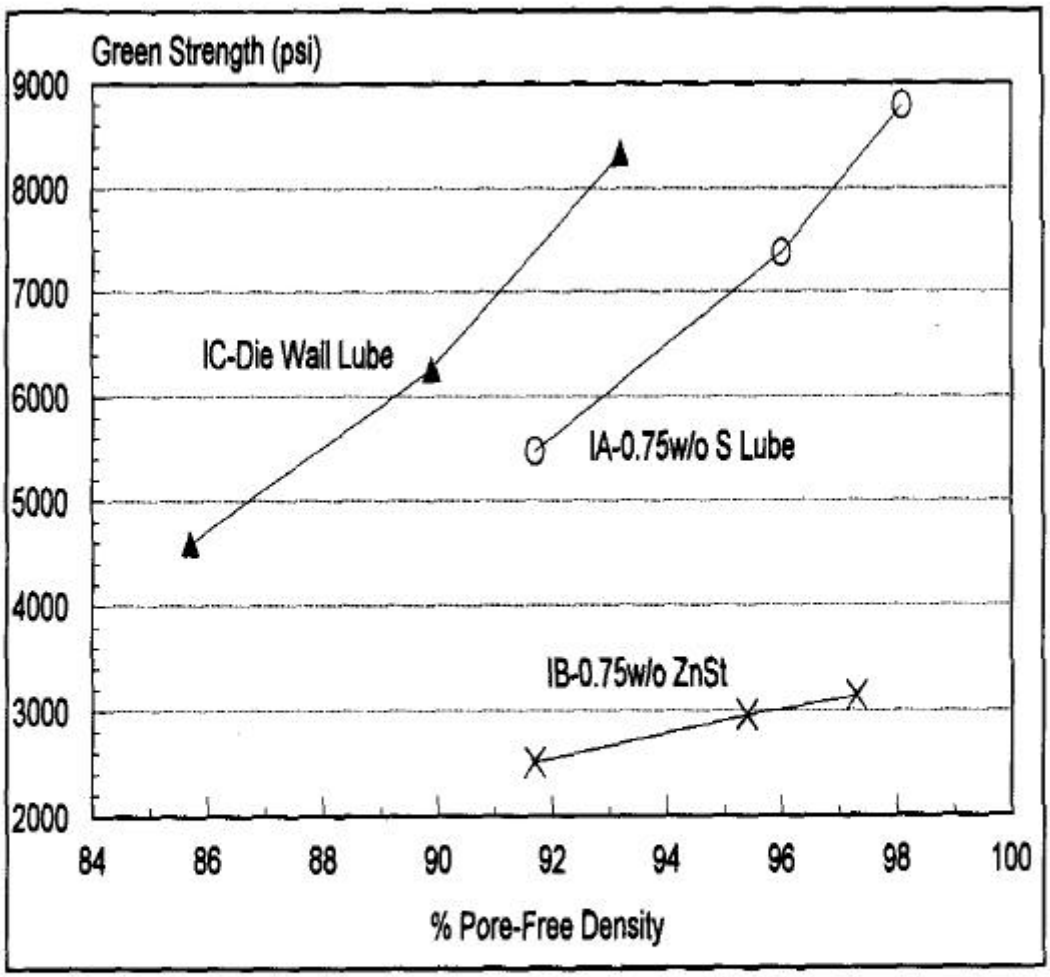

Figure 7: Green Strength as a Function of % Pore-Free Density of Ancorsteel 1000B with 0.75 w/o Admixed S Lube, 0.75 w/o Admixed ZnSt, and Die-Wall Lubricant, Compacted at 30, 40, 50 tsi.

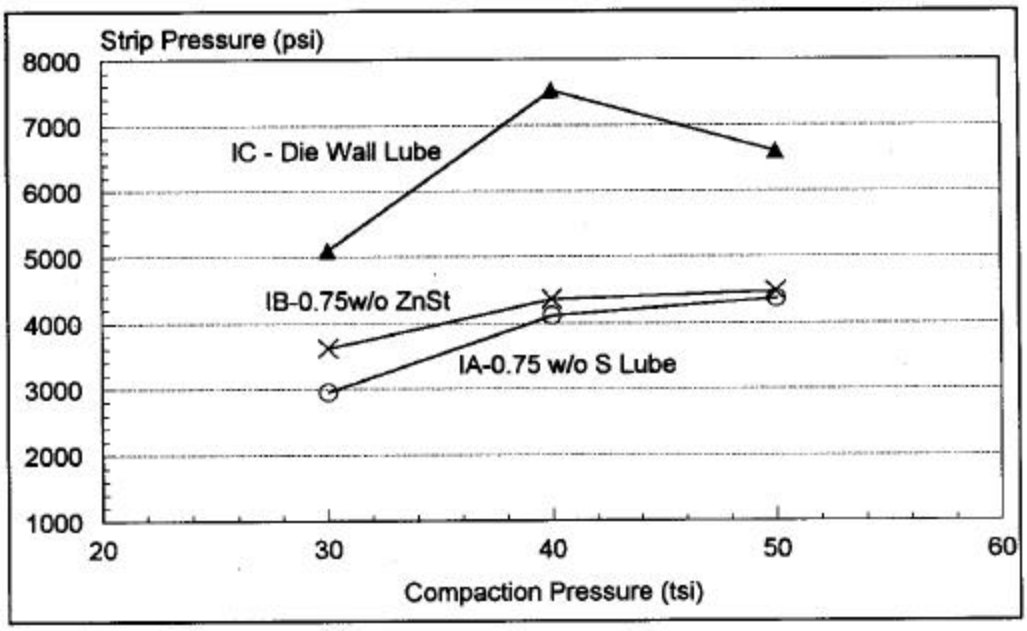

Figure 8: Stripping Pressure of Ancorsteel 1000B with 0.75 w/o Admixed S Lube, 0.75 w/o Admixed ZnSt, and ZnSt Die-Wall Lubricant, Compacted at 30, 40 and 50 tsi.

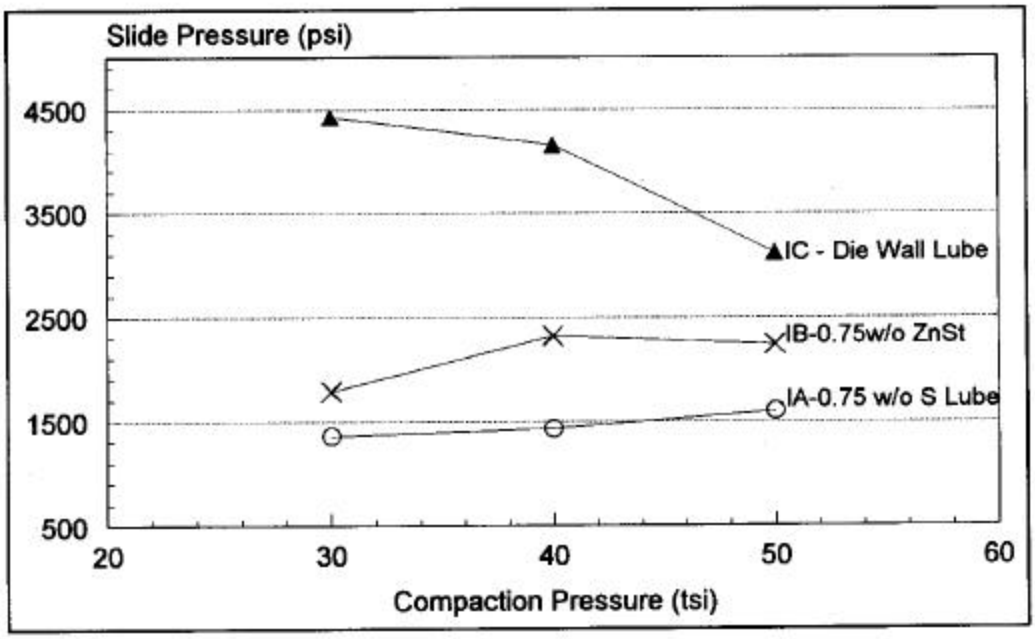

Figure 9: Sliding Pressure of Ancorsteel 1000B with 0.75 w/o Admixed S Lube, 0.75 w/o Admixed ZnSt, and ZnSt Die-Wall Lubricant.

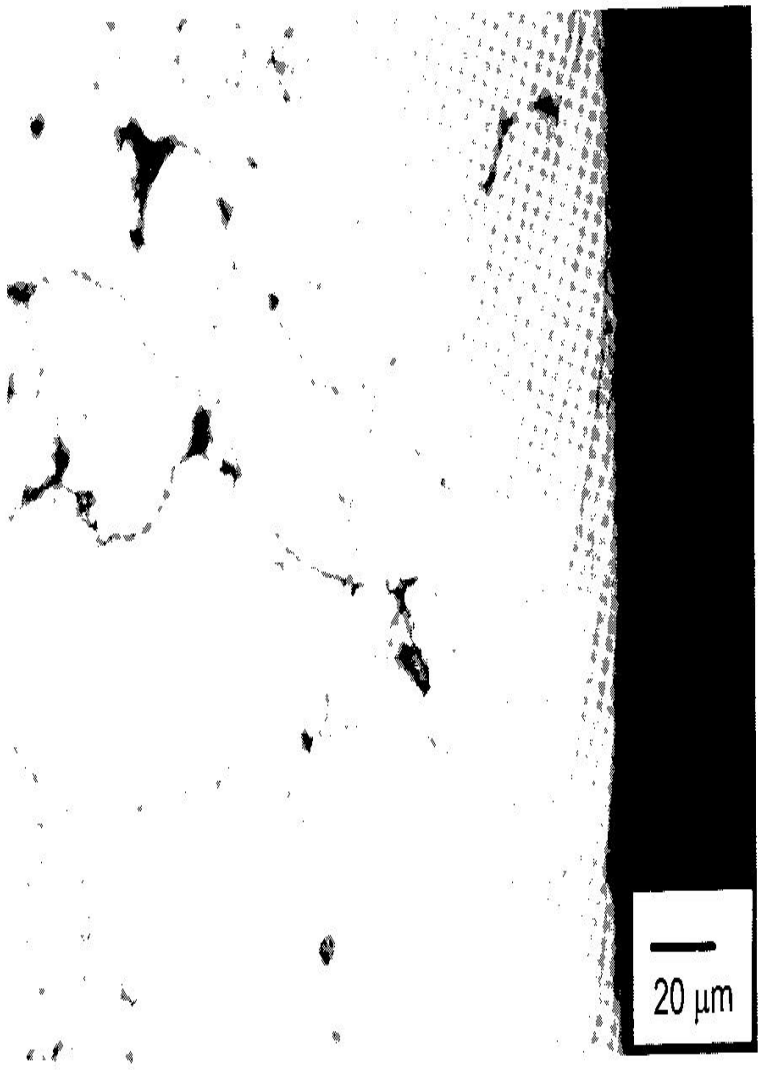

Figure 10: Microstructure of Green Compact Near Die-wall for Material IC-Unlubricated Powder with Die-Wall Lubrication Using Zinc Stearate

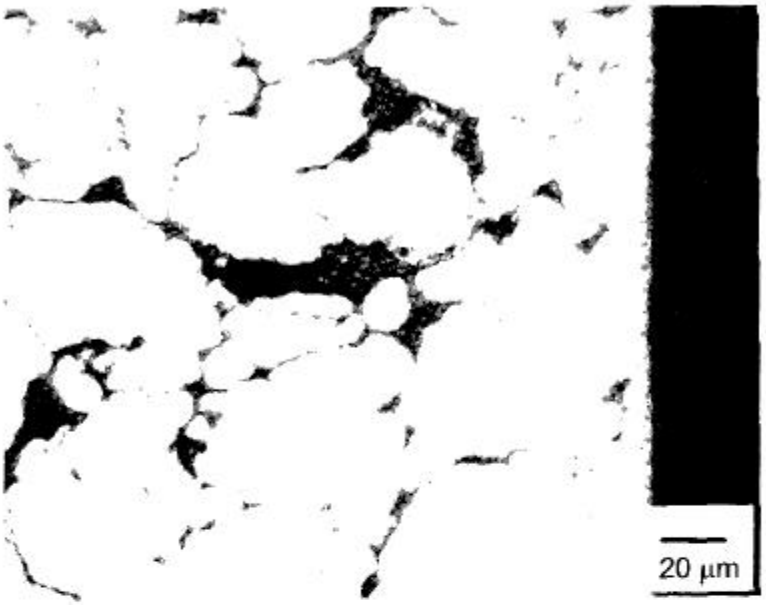

Figure 11: **Microstructure of Green Compact near Die-Wall for Material IB-Lubricated Powder with 0.75 w/o Admixed Zinc Stearate**

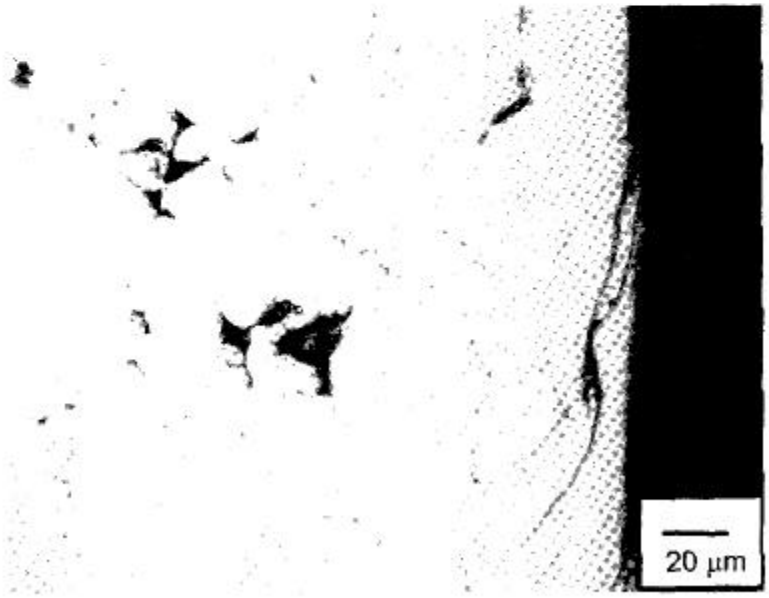

Figure 12: **Microstructure of Green Compact near Die-Wall for Material IA-Lubricated Powder with 0.75 w/o Admixed S Lubricant**

Figure 13: **Microstructure of Green Compact for Material IB Showing Location of Zinc Stearate Between Particle Surfaces.**

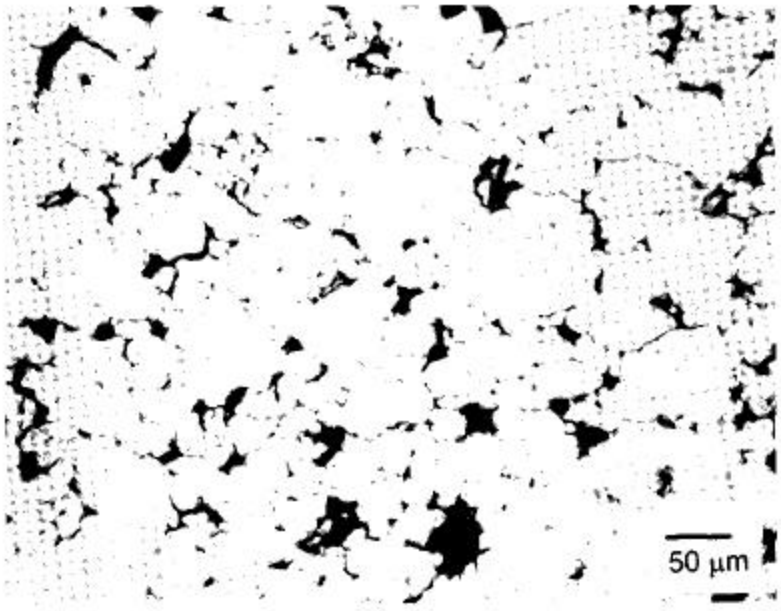

Figure 14: **Microstructure from the Center of Green Compact for Material IC-Unlubricated Powder with Die-Wall Lubrication using Zinc Stearate**

16

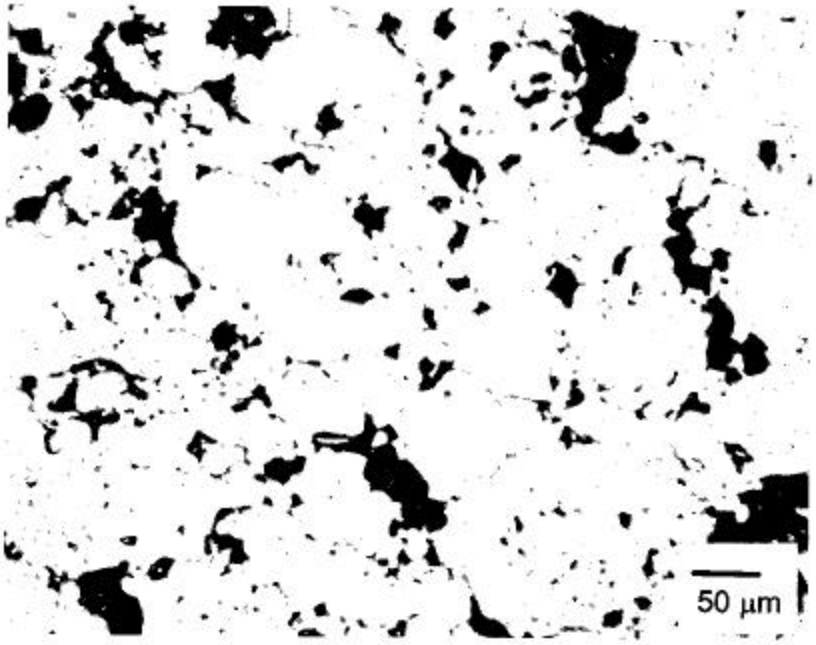

Figure 15: **Microstructure from the Center of Green Compact for Material IB-Lubricated Powder with 0.75 w/o Admixed Zinc Stearate**

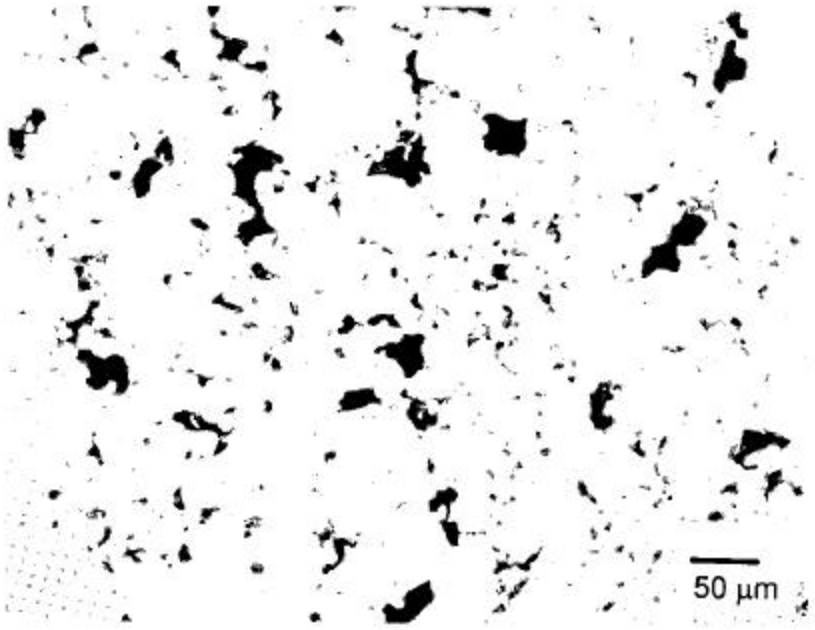

Figure 16: **Microstructure from the Center of Green Compact for Material IA-Lubricated Powder with 0.75 w/o Admixed S Lube**

Table IV: Sintered Properties

Material	Compaction Pressure (tsi)	Sintered Density (g/cm^3)	Dimensional Change (%)	Transverse Rupture Strength (psi)	Apparent Hardness
IA	30	6.82	-0.03	60603	41 (HRF)
	40	7.12	-0.01	75435	55 (HRF)
	50	7.27	+0.01	80469	61 (HRF)
IB	30	6.85	+0.02	66089	42 (HRF)
	40	7.11	+0.02	77613	55 (HRF)
	50	7.26	-0.01	104336	61 (HRF)
IIA	30	6.76	+0.28	142301	77 (HRB)
	40	6.98	+0.39	159839	83 (HRB)
	50	7.07	+0.41	169043	85 (HRB)
IIB	30	6.80	+0.22	150067	77 (HRB)
	40	7.00	+0.26	175144	84 (HRB)
	50	7.09	+0.31	188575	86 (HRB)
IIIA *	50	6.86	-1.28	220769	91 (HRB)
IIIB *	50	6.93	-1.14	225899	99 (HRB)

Sintering Conditions: 2050°F, 30 min., 75v/oH_2 / 25v/o N_2

*410L S/S, Sintering Conditions: 2300°F, 30 min., 75v/oH_2 / 25v/o N_2

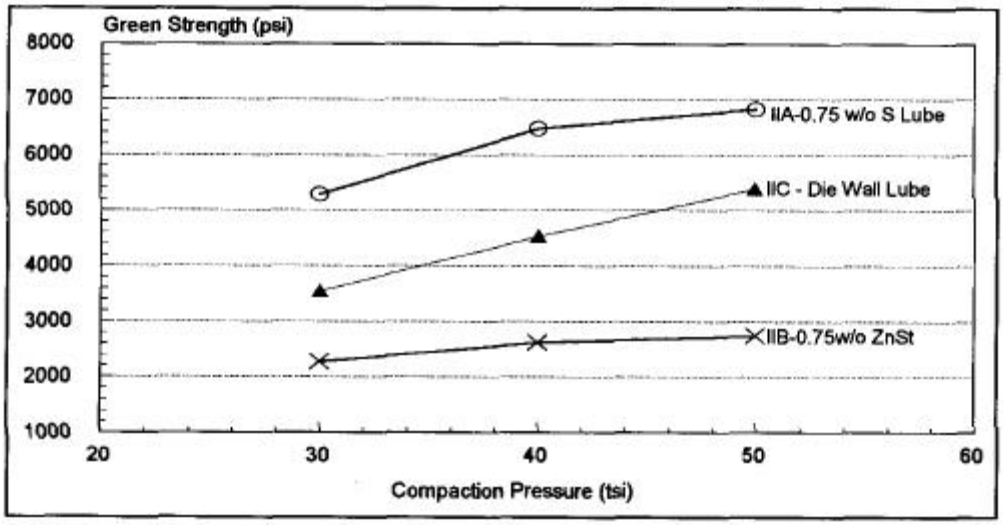

Figure 17: Green Strength of FC-0208 Materials with 0.75 w/o Admixed S Lube, 0.75 w/o Admixed ZnSt, and ZnSt Die-Wall Lubricant.